

Article

Local Structure Analysis on Si-Containing DLC Films Based on the Measurement of C K-Edge and Si K-Edge X-ray Absorption Spectra

Kazuhiro Kanda ^{1,*}, Shuto Suzuki ¹, Masahito Niibe ¹, Takayuki Hasegawa ^{1,2}, Tsuneo Suzuki ³ and Hedetoshi Saitoh ³

¹ Laboratory of Advanced Science and Technology for Industry, University of Hyogo, 3-1-2 Koto, Kamigori-cho, Ako-gun, Hyogo 678-1205, Japan

² Synchrotron Analysis L.L.C., 3-2-24 Wadamaya-dori, Hyogo-ku, Kobe 652-0884, Japan

³ Graduate School of Engineering, Nagaoka University of Technology, 16031-1 Kamitomioka, Nagaoka, Niigata 940-2188, Japan

* Correspondence: kanda@lasti.u-hyogo.ac.jp; Tel.: +81-791-58-0476

Received: 2 March 2020; Accepted: 29 March 2020; Published: 30 March 2020



Abstract: In this paper, the local structure of silicon-containing diamond-like carbon (Si-DLC) films is discussed based on the measurement of C K-edge and Si K-edge near-edge x-ray absorption fine structure (NEXAFS) spectra using the synchrotron radiation of 11 types of Si-DLC film fabricated with various synthesis methods and having different elemental compositions. In the C K-edge NEXAFS spectra of the Si-DLC films, the σ^* band shrunk and shifted to the lower-energy side, and the π^* peak broadened with an increase in the Si content in the Si-DLC films. However, there were no significant changes observed in the Si K-edge NEXAFS spectra with an increase in the Si content. These results indicate that Si–Si bonding is not formed with precedence in Si-DLC film.

Keywords: Si-containing diamond-like carbon film; near-edge X-ray absorption fine structure; dependence on the elemental composition

1. Introduction

Diamond-like carbon (DLC) film is amorphous carbon (a-C) film, which has a disordered form of C consisting of sp^2 and sp^3 hybridized bonds [1,2]. DLC films are widely used as coating materials in various industrial fields due to their superior properties, such as their high hardness, low friction coefficient, chemical inertness, and gas barrier [3–5]. Over the last two decades, various novel DLC films have been synthesized for several industrial purposes. Hetero-atom-containing DLC films were developed because the existence of hetero-atoms in DLC film has the potential to improve the film properties. In particular, the incorporation of Si into DLC films has resulted in an increase in thermal stability [6,7] and resistance to oxidation [8,9], and a decrease in friction in a humid atmosphere [10–12] and intrinsic stresses [13,14]. Therefore, silicon-containing DLC (Si-DLC) films have attracted an increasing amount of attention in various industrial fields due to these properties [15–18].

Near-edge X-ray absorption fine structure (NEXAFS) spectroscopy using synchrotron radiation is known to be sensitive to the local structure around the absorber atom. In near-edge X-ray absorption fine structure (NEXAFS) spectroscopy, the out-coming current from the sample is recorded as a function of the photon excitation energy around the core level of the target element using synchrotron radiation. Transitions occurring via the unoccupied states of the x-ray absorbing elements, whose energy shifts are large, can be observed in this technique. Therefore, NEXAFS is known to be sensitive to the local structure around the absorber atom, in comparison with other spectral evaluation methods. It also does not require long-range ordering and is sensitive to the local bonding structure. Therefore, NEXAFS

spectroscopy is an adequate method for evaluating DLC films, which have an amorphous structure. The NEXAFS spectra of Si-DLC films have also been measured, e.g., C K-edge NEXAFS spectra [19–23] and Si K-edge NEXAFS spectra [24,25]. We previously reported a comprehensive analysis on Si-DLC films based on the measurements of C K-edge NEXAFS spectra [26]. In the present study, we measured the C K-edge NEXAFS spectra and Si K-edge NEXAFS spectra of 11 types of Si-DLC film fabricated using various synthesis methods. The elementary analysis was conducted using a combination of Rutherford backscattering spectrometry (RBS) and elastic recoil detection analysis (ERDA). We discuss the composition ratio of Si dependency on the local structure and the chemical environments of C and Si in Si-DLC films.

2. Materials and Methods

We analyzed 11 types of Si-DLC film, which were provided by enterprises, public organizations, and universities, by measuring the C K-, Si K-, and Si L-edge NEXAFS spectra. These DLC samples were collected by the DLC research group in Japan, which has been working on the classification of DLC films [27]. The Si-DLC films were deposited on Si substrates by using various methods, such as physical vapor deposition (PVD) and chemical vapor deposition (CVD). The desired film thickness was 200 nm.

The RBS and ERDA measurements were performed using an electrostatic accelerator (NT-1700HS; Nissin-High Voltage Co., Kyoto, Japan) located at the Extreme Energy-Density Research Institute, Nagaoka University of Technology, Nagaoka, Japan. Details of RBS and ERDA measurements are described in refs. [28–30]. The He⁺ ions accelerated to 2.5 MeV were used as the incident beam at 72° with respect to the normal surface of a sample. In the RBS measurement, a small fraction—~0.1%—of high-energy He⁺ ions elastically scattered by the sample were captured with a solid-state detector (SSD) arranged at 12° with respect to the normal surface of a sample toward the incident beam. RBS was applied to determine the atomic fractions of C and Si in the samples. In the ERDA measurement, the He⁺ ions elastically collided with H atoms in a sample. The H atoms that were ejected from a sample were detected with an SSD placed at 78° to the normal surface of a sample in the opposite direction to the incident beam. RBS and ERDA signals were simultaneously detected and ERDA was applied to determine the atomic fraction of H in the samples. The estimation error of the RBS/ERDA measurement was 0.5 at.%, because the determination of the content was simulated in 1 at.% steps. The obtained elemental compositions of these samples are listed in Table 1. The ratios of Si/(C + Si) in these films ranged from 0.03 to 0.39.

Table 1. Elemental composition of silicon-containing diamond-like carbon (Si-DLC) films obtained from Rutherford backscattering spectrometry (RBS)/elastic recoil detection analysis (ERDA) measurements and the $sp^2/(sp^2 + sp^3)$ ratio estimated from C K-edge near-edge x-ray absorption fine structure (NEXAFS).

Sample	H Content (at.%)	Si Content (at.%)	Si/(C + Si)	$sp^2/(sp^2 + sp^3)$
1	23	2	0.03	0.61
2	22	5	0.07	0.64
3	20	7	0.09	0.55
4	19	7	0.09	0.31
5	22	8	0.11	0.58
6	29	12	0.17	0.50
7	26	15	0.20	0.44
8	27	15	0.21	0.50
9	41	14	0.23	0.16
10	20	18	0.23	0.63
11	33	26	0.39	0.37

NEXAFS measurements were carried out at the NewSUBARU synchrotron facility of the University of Hyogo [31]. The Si K-edge NEXAFS spectra were measured at beamline 05A, where synchrotron radiation provided by a bending magnet was dispersed using a double crystal monochromator (DXM) [32]. The Si K-edge NEXAFS spectra were measured in the energy range from 1830 to 1880 eV using InSb (111) as a dispersive crystal. The Si L- and C K-edge NEXAFS spectra were measured at beamline 09A, where synchrotron radiation provided by an 11-m undulator was dispersed using a varied spacing planer-grating monochromator [33–35]. The Si L-edge and C K-edge NEXAFS spectra were measured in the energy range from 90 to 120 eV and from 275 to 335 eV, respectively. At both beamlines, monochromatized synchrotron radiation was irradiated on the sample at 54.7° (magic angle) with respect to the normal surface of a sample. All NEXAFS spectra were measured with the total electron yield (TEY) mode. The electrons coming from the sample were detected by measuring the current from the earth to the sample, I_s . The intensity of the incident photon beams, I_0 , was measured by monitoring the photocurrent from a gold mesh, which was placed in front of the sample. The absorption signal was obtained by the ratio between the out-going electron intensity from the sample, I_s , and I_0 . In order to support the correctness of the measurements, all NEXAFS spectra of each sample were recorded at a minimum of three locations.

3. Results and Discussion

Figure 1 shows the measured C K-edge NEXAFS spectra of the 11 Si-DLC film samples. The spectra are displayed from the highest (top) to lowest (bottom) Si/(C + Si) ratio. Figure 2 shows the C K-edge NEXAFS spectrum of the Si-DLC film that had the highest content of Si (sample 11), along with those of diamond powder, HOPG, β -SiC powder, and a typical commercial DLC film that was deposited on a 200 nm-thick Si wafer by using the ion plating method. The sharp π^* peak observed at 285.38 eV in the C K-edge NEXAFS spectra of HOPG is ascribed to the $C1s \rightarrow \pi^*$ resonance transition originating from the C=C bonds [36]. The peak of the $C1s \rightarrow \pi^*$ resonance transition was observed at 284.4 eV in the typical DLC film. This peak was not observed in the C K-edge NEXAFS spectra of diamond powder and β -SiC powder. Structural peaks were observed in the 285–310 eV region of the C K-edge spectra of HOPG, diamond powder, and β -SiC powder. The peaks in the spectra of diamond powder and β -SiC powder are ascribed to the $C1s \rightarrow \sigma^*$ resonance transition generated from the C–C bonds and the C–Si bonds, respectively [36–38]. The peaks in the spectra of HOPG are ascribed to the $C1s \rightarrow \sigma^*$ resonance transition generated from the C–C bonds and C=C bonds. In the C K-edge spectra of the DLC film and Si-DLC film, the $C1s \rightarrow \sigma^*$ resonance transition generated from the C–C bonds, C=C bonds, or C–Si bonds was observed as a broad band at about 285–320 eV, because DLC and Si-DLC have amorphous structures.

The spectral profiles of the C K-edge NEXAFS spectra of the Si-DLC films were reported to change along with the ratio of Si/(C + Si) in the films [26]. As the Si/(C + Si) ratio increases in the film, 1) the σ^* band shrinks due to the change from $\sigma(C-C)$ to $\sigma(C-Si)$ and 2) broadening of the π^* peak can be seen due to an increase in the composition ratio of C=C–Si sites.

The $sp^2/(sp^2 + sp^3)$ ratio of carbon atoms in DLC films is the most important information for understanding the properties of such films. This ratio depends on many factors, such as the deposition method and deposition condition. The $sp^2/(sp^2 + sp^3)$ ratio decreases with an increasing H content in DLC film [39]. The absolute $sp^2/(sp^2 + sp^3)$ ratio of C atoms in DLC film can be determined with a high accuracy because the $1s \rightarrow \pi^*$ resonance transition can be separately observed in the C K-edge NEXAFS spectrum [39–41]. The amount of sp^2 hybridized C atoms can be extracted by normalizing the area of resonance corresponding to the $1s \rightarrow \pi^*$ transitions at 285.4 eV with a large section of the spectrum. The absolute $sp^2/(sp^2 + sp^3)$ ratio was determined by comparing it with that from the NEXAFS spectrum of HOPG, which can be regarded as the full construction of sp^2 hybridized C. The $sp^2/(sp^2 + sp^3)$ ratios estimated from the C-K edge NEXAFS spectra of the Si-DLC films are summarized in Table 1. These values are the average $sp^2/(sp^2 + sp^3)$ ratio obtained from C-K edge NEXAFS spectra measured at three locations of each sample. It was reported that the $sp^2/(sp^2 + sp^3)$ ratios of the Si-DLC films gradually

decreased with an increasing Si/(C + Si) ratio in our previous study [26]. It can be considered that Si atoms only coupled to C atoms by single bonding in Si-DLC films. The present results are almost in accordance with this tendency; however, several exceptions, for example, sample 10, were obtained. The $sp^2/(sp^2 + sp^3)$ ratios of carbon films depend on the deposition method, deposition condition, density, and hydrogen content. In sample 10, the $sp^2/(sp^2 + sp^3)$ ratio was considered to be lowered by its high content of hydrogen.

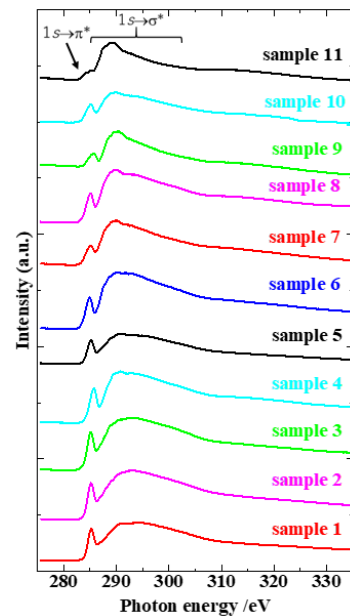


Figure 1. C K-edge NEXAFS spectra of 11 types of Si-DLC film samples. Spectra are displayed from the highest (top) to lowest (bottom) Si/(C + Si) ratio.

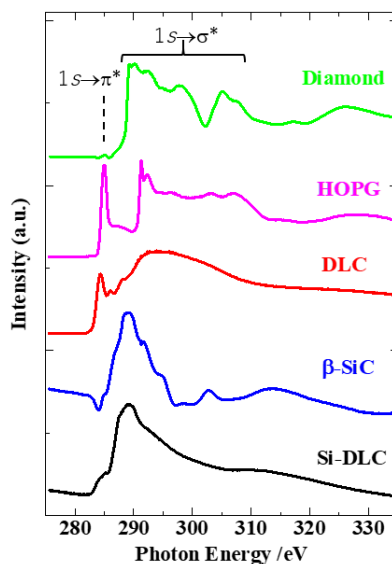


Figure 2. C K-edge NEXAFS spectra of Si-DLC film (sample 11), diamond powder, HOPG, typical DLC film, and β -SiC powder.

Figure 3 shows the Si K-edge NEXAFS spectra of the 11 Si-DLC film samples. The spectra are displayed in the same order as in Figure 1. Figure 4 shows the Si K-edge spectra of sample 11, along with those of SiO_2 powder, β -SiC powder, a-Si:H film, and Si wafer. The energy of the first inflection point, E_0 , and that of the white line, representing an electronic Si $1s \rightarrow t_2$ transition, E_{\max} , depend on the electronegativity of the atoms surrounding the Si [38]. These energies shift towards a higher energy

with an increasing positive charge on the absorber. An intense sharp peak was observed at 1846.8 eV in the spectrum of SiO_2 powder [42]. The E_0 and E_{\max} of the Si-DLC film were slightly higher than those of the Si wafer and a-Si:H film, much lower than those of SiO_2 powder, and similar to those of SiC, as reported by V. Palshin et al. [25]. As shown in Figure 3, E_0 , E_{\max} , and other spectral features did not vary systematically along with the Si/(C + Si) ratio in the present study.

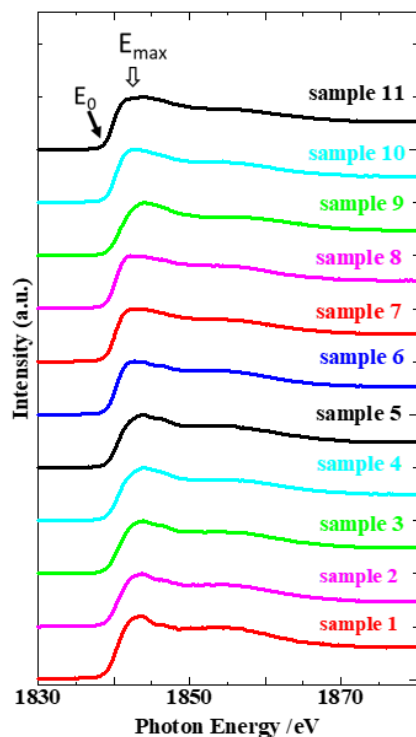


Figure 3. Si K-edge NEXAFS spectra of 11 types of Si-DLC film samples. Spectra are displayed from the highest (top) to lowest (bottom) Si/(C + Si) ratio. A filled arrow and open arrow indicate the position of E_0 and E_{\max} of the Si $1s \rightarrow t_2$ transition, respectively.

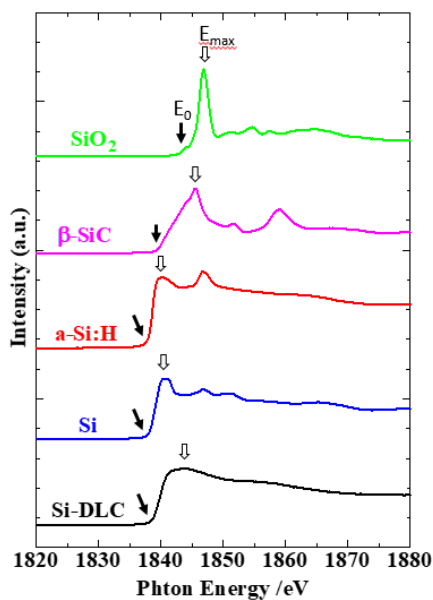


Figure 4. Si K-edge NEXAFS spectra of Si-DLC film (sample 11), SiO_2 powder, β -SiC powder, a-Si:H film, and Si wafer. Filled arrows and open arrows indicate the position of E_0 and E_{\max} of the Si $1s \rightarrow t_2$ transition, respectively.

Figure 5 shows the Si *L*-edge NEXAFS spectra of the 11 Si-DLC film samples. Figure 6 shows the Si *L*-edge NEXAFS spectra of sample 11, along with those of SiO₂ powder, β-SiC powder, a-Si:H film, and Si wafer. In the spectrum of SiO₂, characteristic peaks were observed at 105.4, 106.0, and 107.8 eV, which were assigned to the transitions $2p_{3/2} \rightarrow a_1$, $2p_{1/2} \rightarrow a_1$, and $2p \rightarrow t$, respectively [43]. These characteristic peaks derived from oxidized Si were observed in the Si *L*-edge spectra of samples 3 and 10, as shown in Figure 5, and those of a-Si:H film and Si wafer in Figure 6. These samples were obviously oxidized naturally. However, the characteristic peak derived from oxidized Si, which was observed at 1846.8 eV in the Si *K*-edge spectrum of SiO₂ powder, was not observed in the Si *K*-edge NEXAFS spectra of the above samples. This discordance is ascribable to the difference in the detection depth of Si *K*-edge, with a value of ~1850 eV, and Si *L*-edge, with a value of ~100 eV. Natural oxidation of these samples was considered to occur in the neighborhood of the surfaces of each sample. The energy of the first inflection point, E_0 , of *L*-edge elemental Si is 100 eV and that of silicon oxide is 105 eV [43]. The E_0 of *L*-edge of the Si-DLC films, which are not oxidized, is ~104 eV. This resembled that of SiC, is higher than those of Si wafer and a-Si:H film, and is lower than that of SiO₂ powder. The relation of E_0 positions due to the materials is similar to that in the Si *K*-edge.

As described above, the chemical environment of C atoms varied along with the Si/(C + Si) ratio in the Si-DLC film. However, that of Si atoms was not affected by this ratio. These results indicate that Si atoms in the Si-DLC film dominantly bonded to C atoms in the Si/(C + Si) region, with a value of less than 0.39. In other words, Si–Si bonding did not occur in this Si/(C + Si) ratio region. Palshin et. al. concluded that Si atoms in Si-DLC films are surrounded by four C atoms, as revealed by Si *K*-edge extended x-ray absorption fine structure (EXAFS) measurement [25]. The measurements in the present study agree with their conclusion. However, the Si/(C + Si) ratio of the Si-DLC films they used was 0.125, but that of sample 11 in the present study was ~0.4. In Si-DLC film with an Si/(C + Si) ratio of 0.39, the DLC structure cannot be constructed without coupling of the Si–Si bond. Therefore, the Si *K*- and *L*-edge NEXAFS spectra do not depend on the Si/(C + Si) ratio in Si-DLC films. Additionally, not only do Si atoms tend to enter between C atoms, but the chemical environment of an Si atom coupled to a C atom is close to that of an Si atom coupled to Si atoms, as shown in Figure 4.

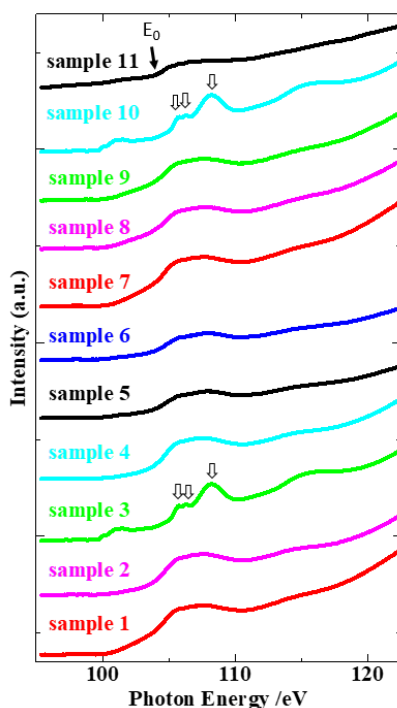


Figure 5. Si *L*-edge NEXAFS spectra of 11 types of Si-DLC film samples. Spectra are displayed from the highest (top) to lowest (bottom) Si/(C + Si) ratio.

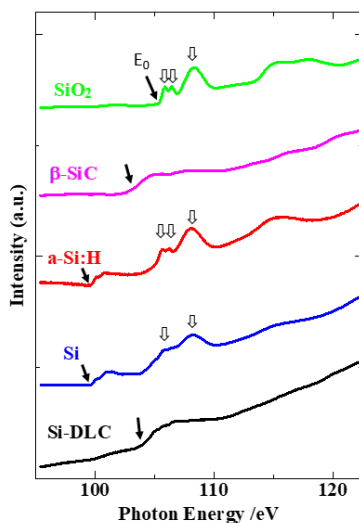


Figure 6. Si L-edge NEXAFS spectra of Si-DLC film (sample 11), SiO₂ powder, β-SiC powder, a-Si:H film, and Si wafer. Filled arrows indicate the position of E_0 . Open arrows indicate the peaks derived from the transitions of the oxidized Si.

4. Conclusions

In this study, we investigated the local structure of Si-DLC films by measuring the C K-edge and Si K-edge NEXAFS spectra of 11 types of Si-DLC film with Si/(C + Si) ratios ranging from 0.03 to 0.39. The spectral features of the C K-edge NEXAFS spectra of the Si-DLC films varied along with the Si/(C + Si) ratio: 1) the σ^* band at 275–335 eV shrank and 2) the π peak at 285 eV broadened. These spectral changes are ascribable to the change from $\sigma(C-C)$ to $\sigma(C-Si)$ and an increase in the composition ratio of C=C–Si sites with the Si/(C+Si) ratio in the Si-DLC films. However, the spectral feature of the Si K-edge NEXAFS spectra of the Si-DLC films did not significantly change along with the Si/(C + Si) ratio. This is considered due to the fact that the Si atom positioned between C atoms in Si-DLC films and/or the chemical environment of an Si atom does not change much between Si–C and Si–Si bonding. Namely, the electronic state of Si in the Si-DLC film is not affected by the Si/(C + Si) ratio.

Author Contributions: Conceptualization, K.K. and S.S.; investigation, K.K., S.S., M.N., T.H., and T.S.; writing—original draft preparation, S.S.; writing—review and editing, K.K.; supervision, H.S.; project administration, K.K.; funding acquisition, K.K. All authors have read and agreed to the published version of the manuscript.

Funding: This research was funded by JSPS KAKENHI, Grant No. JP17K06799, and a Research Grant from the Nippon Sheet Glass Foundation for Materials Science and Engineering.

Acknowledgments: The authors would like to thank Akira Heya of the University of Hyogo for providing the a-Si:H film used as a reference material. We also thank the NewSUBARU staff for their efforts regarding the stable operation of the NewSUBARU ring.

Conflicts of Interest: The authors declare no conflicts of interest. The funders had no role in the design of the study; in the collection, analyses, or interpretation of data; in the writing of the manuscript; or in the decision to publish the results.

References

1. Aisenberg, S.; Chabot, R. Ion-beam deposition of thin films of diamondlike carbon. *J. Appl. Phys.* **1971**, *42*, 2953–2958. [[CrossRef](#)]
2. Robertson, J. Properties of diamond-like carbon. *J. Surf. Coat. Technol.* **1992**, *50*, 185–203. [[CrossRef](#)]
3. Aisenberg, S. Properties and applications of diamondlike carbon films. *J. Vac. Sci. Technol. A* **1984**, *2*, 369–371. [[CrossRef](#)]
4. Grill, A. Diamond-like carbon: State of the art. *Diam. Relat. Mater.* **1999**, *8*, 428–434. [[CrossRef](#)]
5. Robertson, J. Diamond-like amorphous carbon. *Mater. Sci. Eng. R* **2002**, *37*, 129–281. [[CrossRef](#)]

6. Camargo, S.S., Jr.; Santos, R.A.; Baia-Neto, A.L.; Carius, R.; Finger, F. Structural modifications and temperature stability of silicon incorporated diamond-like a-C:H films. *Thin Solid Films* **1998**, *332*, 130–135. [[CrossRef](#)]
7. Wu, W.J.; Hon, M.H. Thermal stability of diamond-like carbon films with added silicon. *Surf. Coat. Technol.* **1999**, *111*, 134–140. [[CrossRef](#)]
8. Camargo, S.S., Jr.; Baia-Neto, A.L.; Santos, R.A.; Freire, F.L.; Carius, R.; Finger, F. Improved high-temperature stability of Si incorporated a-C:H films. *Diam. Relat. Mater.* **1998**, *7*, 1155–1162. [[CrossRef](#)]
9. Kidena, K.; Endo, M.; Takamatsu, H.; Imai, R.; Niibe, M.; Yokota, K.; Tagawa, M.; Furuyama, Y.; Komatsu, K.; Saitoh, H.; et al. Hyperthermal atomic oxygen beam irradiation effect on the hydrogenated Si-doped DLC film. *Trans. Mater. Res. Soc. Jpn.* **2015**, *40*, 353–358. [[CrossRef](#)]
10. Oguri, K.; Arai, T. Tribological properties and characterization of diamond-like carbon coatings with silicon prepared by plasma-assisted chemical vapour deposition. *Surf. Coat. Technol.* **1991**, *47*, 710–721. [[CrossRef](#)]
11. Kim, M.-G.; Lee, K.-R.; Eun, K.Y. Tribological behavior of silicon-incorporated diamond-like carbon films. *Surf. Coat. Technol.* **1999**, *112*, 204–209. [[CrossRef](#)]
12. Chen, T.; Wu, X.; Ge, Z.; Ruan, J.; Lv, B.; Zhang, J. Achieving low friction and wear under various humidity conditions by co-doping nitrogen and silicon into diamond-like carbon films. *Thin Solid Films* **2017**, *638*, 375–382. [[CrossRef](#)]
13. Damasceno, J.C.; Camargo, S.S.; Freire, F.L.; Carius, R. Deposition of Si-DLC films with high hardness, low stress and high deposition rates. *Surf. Coat. Technol.* **2000**, *133*, 247–252. [[CrossRef](#)]
14. Lee, C.S.; Lee, K.R.; Eun, K.Y.; Yoon, K.H.; Han, J.H. Structure and properties of Si incorporated tetrahedral amorphous carbon films prepared by hybrid filtered vacuum arc process. *Diam. Relat. Mater.* **2002**, *11*, 198–203.
15. Lee, K.-R.; Kim, M.-G.; Cho, S.-J.; Eun, K.Y.; Seong, T.-Y. Structural dependence of mechanical properties of Si incorporated diamond-like carbon films deposited by RF plasma-assisted chemical vapour deposition. *Thin Solid Films* **1997**, *308–309*, 263–267. [[CrossRef](#)]
16. Okpalugo, T.I.T.; Ogwu, A.A.; Maguire, P.D.; McLaughlin, J.A.D. Platelet adhesion on silicon modified hydrogenated amorphous carbon films. *Biomaterials* **2004**, *25*, 239–245. [[CrossRef](#)]
17. Kalin, M.; Oblak, E.; Akbari, S. Evolution of the nano-scale mechanical properties of tribofilms formed from low- and high-SAPS oils and ZDDP on DLC coatings and steel. *Tribol. Int.* **2016**, *96*, 43–56. [[CrossRef](#)]
18. Bociaga, D.; Sobczyk-Guzenda, A.; Szymanski, W.; Jedrzejczak, A.; Jastrzebska, A.; Olejnik, A.; Jastrzebski, K. Mechanical properties, chemical analysis and evaluation of antimicrobial response of Si-DLC coatings fabricated on AISI 316 LVM substrate by a multi-target DC-RF magnetron sputtering method for potential biomedical applications. *Appl. Surf. Sci.* **2017**, *417*, 23–33. [[CrossRef](#)]
19. Monteiro, O.R.; Delplancke-Ogletree, M.-P. *Investigation of Non-Hydrogenated DLC: Si Prepared by Cathodic Arc*; LBNL-49944; University of California: Oakland, CA, USA, 2002.
20. Jung, H.-S.; Park, H.-H. Determination of bonding structure of Si, Ge, and N incorporated amorphous carbon films by near-edge x-ray absorption fine structure and ultraviolet Raman spectroscopy. *J. Appl. Phys.* **2004**, *96*, 1013–1018. [[CrossRef](#)]
21. Ray, S.C.; Bao, C.W.; Tsai, H.M.; Chiou, J.W.; Jan, J.C.; Krishna Kumar, K.P.; Pong, W.F.; Tsai, M.-H.; Wang, W.-J.; Hsu, C.-J.; et al. Electronic structure and bonding properties of Si-doped hydrogenated amorphous carbon films. *Appl. Phys. Lett.* **2004**, *85*, 4022–4024. [[CrossRef](#)]
22. Ray, S.C.; Okpalugo, T.I.T.; Papakonstantinou, P.; Bao, C.W.; Tsai, H.M.; Chiou, J.W.; Jan, J.C.; Pong, W.F.; McLaughlin, J.A.; Wang, W.J. Electronic structure and hardening mechanism of Si-doped/undoped diamond-like carbon films. *Thin Solid Films* **2005**, *482*, 242–247. [[CrossRef](#)]
23. Wada, A.; Ogaki, T.; Niibe, M.; Tagawa, M.; Saitoh, H.; Kanda, K.; Ito, H. Local structural analysis of a-SiC_x:H films formed by decomposition of tetramethylsilane in microwave discharge flow of Ar. *Diam. Relat. Mater.* **2011**, *20*, 364–367. [[CrossRef](#)]
24. Mastelaro, V.; Flank, A.M.; Fantini, M.C.A.; Bittencourt, D.R.S.; Carreño, M.N.P.; Pereyra, I. On the structural properties of a-Si_{1-x}C_x:H thin films. *J. Appl. Phys.* **1996**, *79*, 1324–1329. [[CrossRef](#)]
25. Palshin, V.; Tittsworth, R.C.; Fountzoulas, C.G.; Meletis, E.I. X-ray absorption spectroscopy, simulation and modeling of Si-DLC films. *J. Mater. Sci.* **2002**, *37*, 1535–1539. [[CrossRef](#)]
26. Kanda, K.; Niibe, M.; Wada, A.; Ito, H.; Suzuki, T.; Ohana, T.; Otake, N.; Saitoh, H. Comprehensive classification of near-edge X-ray absorption fine structure spectra of Si-containing diamond-like carbon thin films. *Jpn. J. Appl. Phys.* **2013**, *52*, 95504. [[CrossRef](#)]

27. Saitoh, H. Current status on classification work of diamond-like carbon. In Proceedings of the 5th International Conference on New Diamond and Nano Carbons, Matsue, Japan, 16–20 May 2011.
28. Ohkawara, Y.; Ohshio, S.; Suzuki, T.; Ito, H.; Yatsui, K.; Saitoh, H. Dehydrogenation of nitrogen-containing carbon films by high-energy He²⁺ irradiation. *Jpn. J. Appl. Phys.* **2001**, *40*, 3359–3363. [CrossRef]
29. Ohkawara, Y.; Ohshio, S.; Suzuki, T.; Ito, H.; Yatsui, K.; Saitoh, H. Quantitative analysis of hydrogen in amorphous films of hydrogenated carbon nitride. *Jpn. J. Appl. Phys.* **2001**, *40*, 7007–7012. [CrossRef]
30. Igaki, J.; Saikubo, A.; Kometani, R.; Kanda, K.; Suzuki, T.; Niihara, K.; Matsui, S. Elementary analysis of diamond-like carbon film formed by focused-ion-beam chemical vapor deposition. *Jpn. J. Appl. Phys.* **2007**, *46*, 8003–8004. [CrossRef]
31. Ando, A.; Amano, S.; Hashimoto, S.; Kinoshita, H.; Miyamoto, S.; Mochizuki, T.; Niibe, M.; Shoji, Y.; Terasawa, M.; Watanabe, T. VUV and soft X-ray light source “New SUBARU”. In Proceedings of the IEEE Particle Accelerator Conference, Vancouver, BC, Canada, 12–16 May 1997; pp. 757–759.
32. Kanda, K.; Hasegawa, T.; Uemura, M.; Niibe, M.; Haruyama, Y.; Motoyama, M.; Amemiya, K.; Fukushima, S.; Ohta, T. Construction of a wide-range high-resolution beamline BL05 in NewSUBARU for X-ray spectroscopic analysis on industrial materials. *J. Phys. Conf. Ser.* **2013**, *425*, 132005. [CrossRef]
33. Niibe, M.; Mukai, M.; Kimura, H.; Shoji, Y. Polarization property measurement of the long undulator radiation using Cr/C multilayer polarization elements. *AIP Conf. Proc.* **2004**, *705*, 243–246.
34. Niibe, M.; Mukai, M.; Miyamoto, S.; Shoji, Y.; Hashimoto, S.; Ando, A.; Tanaka, T.; Miyai, M.; Kitamura, H. Characterization of Light Radiated from 11m Long Undulator. *AIP Conf. Proc.* **2004**, *705*, 576–579.
35. Kanda, K.; Okada, M.; Kang, Y.; Niibe, M.; Wada, A.; Ito, H.; Suzuki, T.; Matsui, S. Structural changes in diamond-like carbon films fabricated by Ga focused-ion-beam-assisted deposition caused by annealing. *Jpn. J. Appl. Phys.* **2010**, *49*. [CrossRef]
36. Batson, P.E. Carbon 1s near-edge-absorption fine structure in graphite. *Phys. Rev. B* **1993**, *48*, 2608–2610. [CrossRef] [PubMed]
37. Nithianandam, J.; Rife, J.C.; Windischmann, H. Carbon K edge spectroscopy of internal interface and defect states of chemical vapor deposited diamond films. *Appl. Phys. Lett.* **1992**, *60*, 135–137. [CrossRef]
38. Franke, R.; Bender, S.; Jüngerermann, H.; Kroschl, M.; Jansen, M. The determination of structural units in amorphous Si–B–N–C ceramics by means of Si, B, N and C K–XANES spectroscopy. *J. Electron Spectrosc. Relat. Phenom.* **1999**, *101–103*, 641–645. [CrossRef]
39. Saikubo, A.; Yamada, N.; Kanda, K.; Matsui, S.; Suzuki, T.; Niihara, N.; Saitoh, H. Comprehensive classification of DLC films formed by various methods using NEXAFS measurement. *Diam. Relat. Mater.* **2008**, *17*, 1743–1745. [CrossRef]
40. Kanda, K.; Kitagawa, T.; Shimizugawa, Y.; Haruyama, Y.; Matsui, S.; Terasawa, M.; Tsubakino, H.; Yamada, I.; Gejo, T.; Kamada, M. Characterization of hard DLC films formed by Ar gas cluster ion beam-assisted fullerene deposition. *Jpn. J. Appl. Phys.* **2002**, *41*, 4295–4298. [CrossRef]
41. Saikubo, A.; Kanda, K.; Niibe, M.; Matsui, S. Near-edge X-ray absorption fine-structure characterization of diamond-like carbon thin films formed by various method. *New Diam. Front. Carbon Technol.* **2006**, *16*, 235–244.
42. Li, D.; Bancroft, G.M.; Kasrai, M.; Fleet, M.E.; Secco, R.A.; Feng, X.H.; Tan, K.H.; Yang, B.X. X-ray absorption spectroscopy of silicon dioxide (SiO₂) polymorphs: The structural characterization of opal. *Am. Mineral.* **1994**, *79*, 622–632.
43. Sammynaiken, R.; Naftel, S.; Sham, T.K.; Cheah, K.W.; Averboukh, B.; Huber, R.; Shen, Y.R.; Qin, G.G.; Ma, Z.C.; Zong, W.H. Structure and electronic properties of SiO₂/Si multilayer superlattices: Si K edge and L_{3,2} edge X-ray absorption fine structure study. *J. Appl. Phys.* **2002**, *92*, 3000–3006. [CrossRef]



© 2020 by the authors. Licensee MDPI, Basel, Switzerland. This article is an open access article distributed under the terms and conditions of the Creative Commons Attribution (CC BY) license (<http://creativecommons.org/licenses/by/4.0/>).